A Vision Approach for Expiry Date Recognition using Stretched Gabor Features

Ahmed Zaafouri, Mounir Sayadi, and Farhat Fnaiech
Department of Electrical Engineering, University of Tunis, Tunisia

Abstract: *Product-expiry date represent important information for products consumption. They must contain clear information in the label. The expiry date information stamped on the cover of product faced some challenges due to their writing in pencil and distorted characters. In this paper, an automated vision approach for recognizing expiry date numerals of industrial product is presented. The system consists of four stages namely, numeral string pre-processing, numerals string segmentation, features extraction and numeral recognition. In pre-processing module, we convert the image to binary image based on threshold. A vertical projection process is adopted to isolate numerals, in the segmentation module. In the features extraction module, Fourier Magnitude (FM), Local Energy (LE) and Complex Moments (CM) derived from Stretched Gabor (S-Gabor) filters outputs are extracted at various filter orientations. Also, the mean and the variance of each feature map are extracted. The recognition process is achieved by classifying the extracted features, which represent the numeral image, with trained Multilayer Neural Network (MNN) using k-fold cross validation procedure. Through experiments, we demonstrate the richness of the S-Gabor features of information is highlighted. Consequently, the set of features shows its usefulness for practical usage.*

Keyword: *Computer vision, FM, CM, LE, numeral recognition, NN, S-Gabor filters.*

Received March 21, 2013; accepted December 24, 2013; published in September 4, 2014

1. Introduction

In machine vision inspection application, the system must be able to perform successfully label verification [15]. In computer vision inspection system, character verification and recognition is an important research field. There are also many control applications where the products should be identified via numeral codes such as: Product reference, batch number and expiry-date.

In recent years, many researchers related to industrial applications have been developed like: Vehicle license plate recognition [6, 18, 23, 26] and product code inspection as quality control of the label of medical product [24], control of the numeral on pulp bales [10], visa card numeral code reading [7] and check amount recognition [16] and container-code recognition [25]. The product codes are often printed somewhere on the product and presents some difficulties to recognize them. Expiry date of the product is important information for consumer. This information appears such numerical or alphanumerical characters as shown in Figure 1.

Figure 1. Examples of expiry date images.

In the production line, expiry date faces some difficulties due to the pencil stamping method, packaging phase and many others constrains. Also, depending to the storage duration of the product expiry date may be appearing distorted and presenting holes, and the characters can be warped. Too, the character image may be skewed; the thickness and the shape of characters are incoherent. Despite the importance of this information in our daily use, it is not treated before in literature. This paper presents an automated vision approach for product Expiry Date Recognition (EDR). It can be established by a digit series stamped on the cover of the product with different form Figure 1. As all previous works [25], the proposed EDR system is divided into four main modules: Expiry date image preprocessing, expiry date code segmentation, features extraction and finally numerals classification. In the first stage, the input image is binarized using morphological operator. Then, the segmentation is performed using vertical projection. Then, a set of features are extracted from Stretched Gabor (S-Gabor) filters output like Fourier Magnitude (FM), Local Energy (LE) and complex moment with statistical features. Finally, Multilayer Neural Network (MNN) is used to classify the expiry date numeral into ten classes.

The rest of the paper is organized as follows: Section 2 is devoted to present an overview of the proposed method. This section is divided into: The input image binarization, the segmentation of the numeral string, S-Gabor filters design, the features extraction steps and MNN classifier.

Section 3 presents simulation results and discussion demonstrating the performance of the automatic method for numeral classification and recognition. Finally, conclusion is drawn in the last section.

2. Overview of the Proposed Method

After image binarization, the segmentation of digits string is carried out. Then, each normalized digit image is convolved with a bank of S-Gabor filter at some orientations and at specified frequency (*filter* 1, …, *filter* '*o*'; with '*o*' is the number of orientations). According to the number of orientation of the filter, many feature maps are determined. For instance, if '*o*=3' we have three features map of LE and likewise for FM and CM. In each stage of the filtering algorithm, the norm of the difference between feature maps at subsequent orientation channels is calculated and considered. Finally, a vector consisting of many features, depending on the number of orientation, of each numeral is obtained. The feature vector is considered as an input of a MNN for numeral recognition. Figure 2 illustrates the flowchart of the proposed algorithm. In the sequel, let us explain each bloc separately, as drawn in Figure 2.

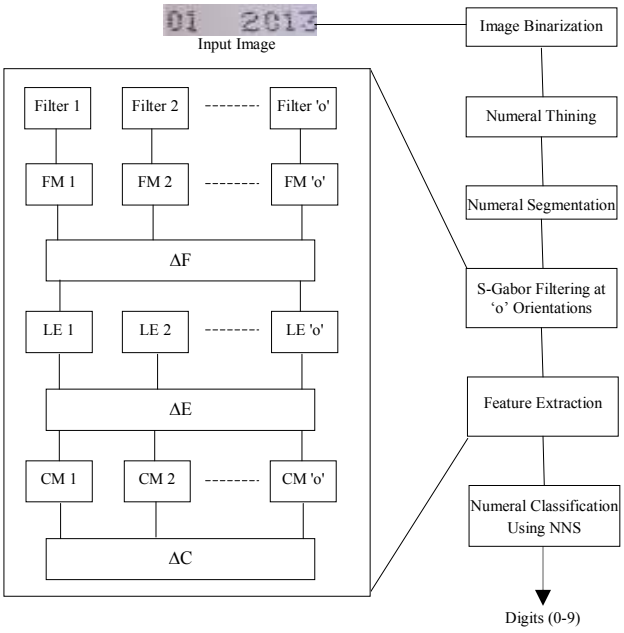

Figure 2. Flowchart of the numeral recognition system.

2.1. Preprocessing of the Expiry Date Images

The preprocessing stage comprises two modules: The binarization of the input image followed by expiry date image thinning. Firstly, the obtained expiry date image is converted to a grayscale *GS* image with the following Equation:

$$GS(image) = 0.2990R + 0.5870G + 0.1140B \quad (1)$$

R, *G* and *B* are respectively, three color components of red, green and blue.

Now, everything is ready for binarization of image, thresholding is employed for binarization of the gray level image and thus to separate the object of interest from the background. After the binarization, the morphological algorithm is employed in the thinning module. The result of the binarization and thinning modules of expiration code without duplication is shown in Figure 3.

a) Original image. b) Grayscale image.

c) Binary image. d) Thinned image using morphological operator.

Figure 3. Binarization of the expiry date images.

In the others words, some shortcomings could corrupt the expiration code such as connected characters, overlapping and skewed code. The touching numerals problem is in general due to the digit thickness and skewed code is due to the positioning of the product towards the camera and so captured image requires skew correction. The two problems are considered in the following.

In our paper connected numerals and skewed code are considered. For the skewed code Figure 4-a, the gradient based algorithm [21] is applied for skew correction. This approach performs as follows: The gradient of the input image is estimated using sobel operator and the orientation histogram is smoothed using median filter. The maximum of the histogram represents the initial skew angle. Also, the skew angle is determined by the difference between $\pi/2$ and the initial skew angle. After skew correction, the image is binarized and digits are extracted.

The second problem treated in our paper is given by touching numerals due to their thickness as shown in Figure 5. The input image is binarized using specified thresholding value and in order to reduce connected component, the binary image is convolved with the filter kernel *h* given by:

$$h(x,y) = \begin{bmatrix} 0 & 0 & 0 & 0 & 0 \\ 0 & 1 & 1 & 1 & 0 \\ 0 & 1 & 1 & 1 & 0 \\ 0 & 1 & 1 & 1 & 0 \\ 0 & 0 & 0 & 0 & 0 \end{bmatrix} \quad (2)$$

The result of the convolution $Ic(x, y)$ is binarized again and thinned and the numerals are segmented by vertical projection technique. Figure 5 shows the process of numerals separation.

a) Skewed expiry code. b) Skew corrected image.

Figure 4. Skew angle correction.

a) Expiration code with touching numerals.

b) Convolution results Ic(x, y).

c) Binarized code image.

Figure 5. Processing of connected numerals.

2.2. Expiry Date Numerals Segmentation

After expiration code pre-processing, the next stage in our recognition process consists of the segmentation of digits string. The vertical projection technique is the well known method to extract character images. It is widely used in character segmentation and especially for fragmented written character [18]. It is the histogram $h(x)$ obtained by counting of black bits in each vertical scan at position x. In a single line vertical projection, a peak occurs for each stroke of the numeral. This technique demonstrates that the numerals are well separated because the histogram has zeros values between numerals as shown in Figure 6.

Figure 6. Segmentation of expiry date code. From top to down: Original image, binary image, thinned image, segmented expiry date numerals.

2.3. 2D S-Gabor Filters Design

After the segmentation process, each normalized numeral image is convolved with a bank of 2D S-Gabor filters [11]. The filter is constructed in the frequency domain and it can be divided into two components: The radial and the angular filter. The even filter has a frequency response described by [17].

$$G_r(r,\theta)=\left[e^{-r^2/2\sigma^2}.\cos(2\pi f_0 r\zeta(r))\right]\times\cos^{2m}(\theta_0-\theta) \quad (3)$$

The cosine function in Equation 3 is replaced by the sine function in order to obtain odd symmetric S-Gabor filter. The filter given by Equation 3 suffers some drawbacks as the blurred effect introduced in the LE map and the false response to 1D features [17]. To reduce the blurred effect of the LE and the false response to 1D image features, the angular component given in Equation 3 by a power of cosine function is replaced and the S-Gabor filter is expressed by:

$$G_r(r,\theta)=\frac{1}{2}\times\left[e^{(-r^2/2\sigma^2)}.\cos(2\pi f_0 r\zeta(r))\right]\times(\cos(\theta_0-\theta)+|\cos(\theta_0-\theta)|)^{2m} \quad (4)$$

Where σ determines the width of the gaussian envelope, m is a constant parameter determining orientation selectivity of the filter, f_0 is the frequency at the origin, θ_0 denote the orientation angle of the filter and $\xi(r)$ gives the frequency sweep of the filter, it is expressed by:

$$\zeta(r)=1/2.\left(e^{-\lambda(r/\sigma)^2}+1\right) \quad (5)$$

Where λ is chosen numerically so that, the even S-Gabor function integrates to zero and r denote the polar coordinates. In our experiments, the parameters are set to σ=2; m=2, the center frequency f_0 is chosen equal to 0.1 and λ=0.5. These parameters are set in order to give thin feature responses and reduce the blur effect on local energy, FM and CM response and consequently in order to obtain successfully performance of the proposed algorithm.

The bracketed expression in Equation 4 represents the radial component shown in Figure 7-a and the power of cosine express the angular component as shown in Figure 7-b. The two components are multiplied together to construct the overall S-Gabor filter $G_r(r, \theta)$ as illustrated in Figure 7-c.

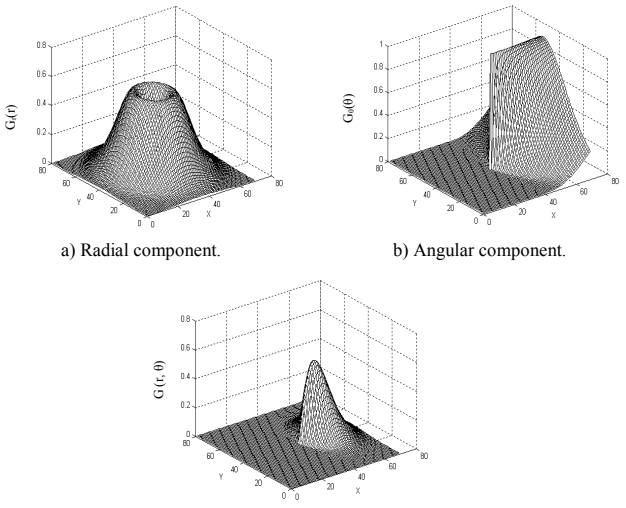

a) Radial component.

b) Angular component.

c) Resulting filter with f_0=0.1, λ=0.5, σ=2 and m=2.

Figure 7. The 3D representation of the three components of 2D S-Gabor filters.

2.4. Features Extraction

2.4.1. Fourier Response Features

The convolution of the image with a bank of filters gives a set of features used for texture and image analysis. Gabor filters bank is the well used in this area. The magnitude response has been used for texture classification [4]. Also, only the real components were used for texture segmentation [12].

The imaginary component derived from gabor filter output is used for handwritten numeral recognition [22]. The magnitude response is used as features in our study.

The input numeral image $I(x, y)$ is convolved, in the frequency domain, with a bank of S-Gabor filters $G_r(r, \theta)$. The magnitude response at each orientation 'o' is expressed as follows:

$$A_O(x,y) = \left| \mathcal{F}^{-1}[\mathcal{F}(I(x,y)) \times \mathcal{F}(G_r(r,\theta))] \right| \quad (6)$$

Where $\mathcal{F}$ is the fourier transform and $\mathcal{F}^{-1}$ denote the inverse fourier transform. The FM is computed at each orientation channel. The norm of the difference between subsequent FM ΔA is computed giving a first feature used in the recognition process. The mean and the variance of each FM response at orientation channel are calculated.

2.4.2. LE Features

In this work, we exploit the S-Gabor filters properties for LE computation. The LE is computed over various orientations. The LE at each orientation 'o' is computed by [14]:

$$E_o^L(x,y) = W(x) \lfloor A_o(x,y) \Delta\phi_o(x,y) - T \rfloor \quad (7)$$

Where $w(x)$ is the sigmoid function used to weight LE, $\Delta\phi_o(x, y)$ is a phase deviation measure, $A_o(x, y)$ is the FM response, the symbols $\lfloor \rfloor$ denote the enclosed quantity is equal to itself when its value is positive and zero. Otherwise, this LE measure is interesting to takes into account the noise cancelation. According to [14], the noise compensation term is expressed by:

$$T = \mu_R + k\,\sigma_R \quad (8)$$

Where μ_R is the mean noise response and σ_R is the standard deviation and k is a constant value chosen between 2 and 3.

In our case the constant k is equal to 3. The total energy $E^T(x, y)$ is given by taking the summation of the LE for all orientations. The total energy is given by:

$$E^T(x,y) = \sum_o E_o^L(x,y) \quad (9)$$

Figure 8 shows the LE features map at different orientation of two numerals.

a) The segmented numeral.

b) From left to right the LE feature map at four filter orientations (θ=0º, π/4, π/2, 3π/4).

Figure 8. The LE features map of two numerals.

The relation between the local power spectrum and the S-Gabor energy features can be defined by:

$$P_o(x,y) = (E_o^L(x,y))^2 \quad (10)$$

For a given image, the LE is evaluated for each pixel and at each orientation. The norm of the difference between two subsequent energy feature maps at orientation channels, ΔE is calculated. Equally, we compute at each orientation channel the mean and the variance of the LE feature map.

2.4.3. Complex Moment Features

The complex moment of a function $f(x, y)$ is defined by [3]:

$$I_{mn} = \int\int (x+iy)^m (x-iy)^n f(x,y)\,dx\,dy \quad (11)$$

Where $m, n \in \mathbb{N}$

In image processing applications, the complex moments are used as features descriptors of textured images. Therefore, the real and imaginary parts of the complex moments of the local power spectrum were proposed as features that give information about the presence or absence of dominant texture orientations. The sum $(m+n)$ called the order of the complex moment is related to the number of dominant orientations in the texture [20].

The complex moments of the local power spectrum at orientation 'o' may be estimated by:

$$C_o^{mn}(x,y) = \sum_{x=1}^{M} \sum_{y=1}^{N} (x+iy)^m (x-jy)^n P_o(x,y) \quad (12)$$

With $P_o(x, y)$ denote the local power spectrum given by Equation 8.

In the sequel, we compute the estimated complex moment at each orientation channel and at each pixel by using Equation 12. The computed complex moments are complex quantities, their magnitudes give information about the presence or absence of dominant orientations while their arguments specify which orientations are dominant [20]. The order of the complex moments is chosen equal to 1 (i.e., $m+n=1$). For $m=1$, $n=0$ and if $m=0$, $n=1$. All cases are taken account.

At each pixel, the magnitude of the complex moment of order 1 at orientation 'o' is given by:

$$C_o^1(x,y) = \sqrt{(Re(C_o^1(x,y)))^2 + (Im(C_o^1(x,y)))^2} \quad (13)$$

Where $Re(C_o^1(x, y))$ and $Im(C_o^1(x, y))$ are the real and imaginary parts of the complex moment at orientation 'o', respectively. Figure 9 shows the magnitude of the complex moments features map of two numerals at four filters orientations.

For a given image, the magnitude of the complex moments of order 1 is computed for each orientation. Then, an important features ΔC^1 representing the norm of the difference between two subsequent C_o^1 and C_{o+1}^1 orientation channel is calculated. Also, the mean and the variance of the complex moment feature map, at each orientation channel C_o^1 are calculated and used as features.

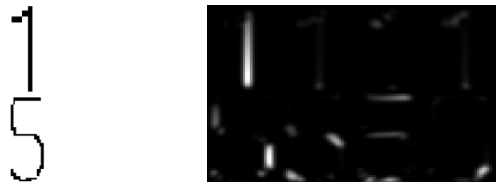

a) Segmented numeral.

b) From left to right the complex moment feature maps at four filter orientations (θ=0°, π/4, π/2, 3π/4).

Figure 9. The magnitude of the complex moment's features map of Arabic numeral.

2.4.4. Numeral Straight-Line and Curve Main Features Indexes

After defining, in the previous sections, the FM $A_o(x, y)$, the LE $E_o^L(x, y)$ and the magnitude of the complex moments $C_o^1(x, y)$ at each orientation, now these quantities may be used to compute the main digit straight line and curves features such as ΔE_n, ΔA_n and ΔC_n.

Following [5], the norm of the difference between LE feature maps, at subsequent orientation channels, is calculated. The first norm of difference between subsequent LE is given by:

$$\Delta E_n = \left\| E_n - E_{n+1} \right\| \quad (14)$$

Also, we compute the norm of the difference between subsequent magnitude responses

$$\Delta A_n = \left\| A_n - A_{n+1} \right\| \quad (15)$$

In the same way we compute the norm of the difference between subsequent complex moments magnitude of order 1 as follows:

$$\Delta C_n^1 = \left\| C_n^1 - C_{n+1}^1 \right\| \quad (16)$$

Where E_n, A_n and C_n^1 are the local energy, the FM and the first order complex moments magnitude features map at orientation n, (n=1, …, 3).

Table 1 illustrates the main local energy, FM and complex moment features indexes of three numerals. The extracted features indexes of FM spectrum and complex moments can be calculated in the same manner using Equations 15 and 16, respectively. It is well shown that features of digit '6' and '5' are distributed equally in all orientations channel. For the numeral '1', the FM, LE and complex moments are concentrated in the single orientation channel with some leakage into adjacent neighboring channels [5]. Here of, the numerals can be classified into two classes. The first class is called curved numeral and the second is linear numeral. Figure 10 shows that for numeral '1' the LE features index is concentrated in the first channel, likewise for the complex moment features index in Figure 10-b. While for numerals '5' and '6', the features indexes are distributed equally at orientation channel. Furthermore, for the numerals containing dominant linear features the value ΔE_1 is far from ΔE_2 and ΔE_3 ('numeral 1' in Table 1) while the value ΔE_1 is close to ΔE_2 and ΔE_3 for the digits composed by curve features ('numeral 5 and 6' in Table 1). Likewise the same interpretations of LE features indexes can be extended for complex moments and FM feature indexes as shown in Table 1.

Table 1. The features indexes of three numerals for four filter orientations.

Feature Indexes	Numeral '1'	Numeral '5'	Numeral '6'
$\Delta E_1 = \left\| E_1 - E_2 \right\|$	404.82	242.36	332.41
$\Delta E_2 = \left\| E_2 - E_3 \right\|$	128.25	299.88	289.83
$\Delta E_3 = \left\| E_3 - E_4 \right\|$	125.74	313.87	334.42
$\Delta A_1 = \left\| A_1 - A_2 \right\|$	432.07	257.05	352.50
$\Delta A_2 = \left\| A_2 - A_3 \right\|$	149.49	276.45	304.07
$\Delta A_3 = \left\| A_3 - A_4 \right\|$	148.07	307.28	335.95
$\Delta C_1^1 = \left\| C_1^1 - C_2^1 \right\|$	7.07e+005	4.30e+005	5.34 e+005
$\Delta C_2^1 = \left\| C_2^1 - C_3^1 \right\|$	0.59e+005	3.40e+005	4.94e+005
$\Delta C_3^1 = \left\| C_3^1 - C_4^1 \right\|$	0.60e+005	3.53e+005	5.03e+005

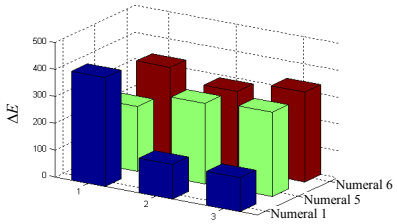

a) The LE feature indexes.

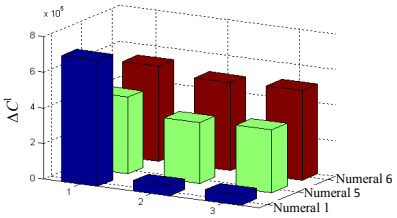

b) The complex moment feature indexes.

Figure 10. Linear and curve main features indexes of three numerals.

2.5. Multilayer NN Classifier

To recognize segmented character, numerous methods from Support Vector Machine (SVM) to Neural Network (NN) have been investigated. From these methods those using self organized NN [6], Probabilistic Neural Network (PNN) [2], Artificial Neural Network (ANN) [13], Hidden Markov Model (HMM) [8] and SVM [9, 19] and K-Nearest Neighbor (KNN) [1]. The neural networks are well methods adopted in character recognition. Here, in MLP NN is adopted. Also, MLP is established, with one hidden layer, which learns with the error back-propagation procedure, for classifying and recognizing numerals. When the learning is stopped, the NN is then ready for the generalization procedure. The input database provided for training the NN contains 100 samples images for each expiry date number.

Several iterations are required to train the network, but once it is trained, it is fit for classifying unknown vectors and assigns each one to a specific numerals class [22]. Figure 11 illustrates the general MNN architecture used for numeral recognition.

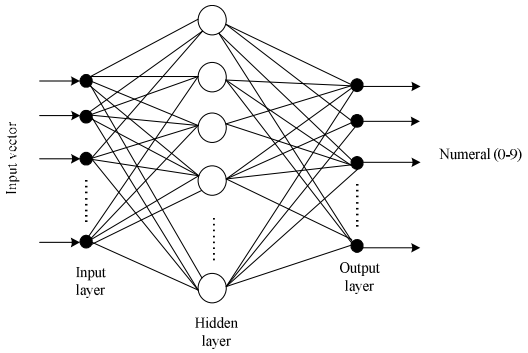

Figure 11. MNN classifier architecture.

3. Experimental Results

In this section, we demonstrate the importance of the features derived from S-Gabor filter output for expiry date numeral recognition. The database used in our experiments consists of 2000 photos of product label under different illumination and various numerical format of expiry date. Only numerical expiry date images are considered, in our study. The segmented and normalized numeral images with size 50×30 are used. We have 100 samples for each digit class so in total 1000 samples. To obtain uniformity in generating the recognition accuracy, input data are divided into 5-folds.

In order to measure the performance of our algorithm on the numerals recognition problem, 5-fold cross validation procedure is used. The principle of this method consists to divide the dataset in 5 disjoint sets. The main advantage of using k-fold cross validation is that all examples in the dataset are eventually used for both training and testing. In our experiments, 5-fold cross validation technique is used and the performance of the algorithm of each fold is determined. The overall performance is determined by the average of the five folds accuracy.

The set of features used in our experiments are given by a variable numbers of features indexes (Table 1) with the mean and the standard deviation of each feature map. For instance, for four filter orientations (θ_o=0º, π/4, π/2, 3π/4), 9 feature indexes for each numeral are extracted as demonstrated in Table 1. In addition, the mean and the standard deviation at each orientation channel gives 24 features (8 for LE, 8 for CM and 8 for FM) for each numeral image. The feature vector is composed by 33 features in total, in our experiments. Also, the performance of the recognition system is tested over various filter orientations as shown in Table 2. The extracted features are used as input of multilayer NN having better configuration.

Table 2. Average recognition rate (%) of the proposed algorithm using 5-fold cross validation.

Number of Features	Average Recognition Rate (%)
33 Input Features (o=4)	99.3
42 Input Features (o=5)	99.1
51 Input Features (o=6)	98.7
69 Input Features (o=8)	98.5

The constructed NN has one hidden layer with 50 neurons and the learning rate is set to 0.1. These parameters are reached by try and error and also by trade-off between two parameters of consuming time and the recognition accuracy. The number of the input nodes is variable according to the number of orientation of the filter. The number of the output of the network is equal to 10 corresponding to the number of the numeral (0-9). In order to train the MNN classifier we adopted the back propagation algorithm. Learning was terminated when the mean square error is lower. Here, the maximum number of iterations was set to 5000. Table 2 illustrates the average recognition rate of the proposed algorithm using different number of input features using five folds cross validation. We show that for four orientations, the proposed algorithm gives a higher recognition rate. Also, if we use 8 orientations the angular bandwidth between successive orientation channels is well small and the norm of the difference (see Table 2) between feature indexes is not well distinguished.

The performance of the S-Gabor features depends typically on parameters of the filter m, λ and σ. The parameter m defines the orientation selectivity of the filter. The parameter σ determines the width of the gaussian envelope and λ determines the frequency spread of the filter. Also, if σ increases all features response are thicker. So, the difference between subsequent feature maps presents leakages and the recognition rate of the proposed algorithm decreases. The parameter m defining the orientation selectivity of the filter must be chosen small in order to guaranties high recognition rate. This parameter does not a large influence in the output results by using new angular component of the S-Gabor filter. An appropriate selection of the parameter λ in the sweep function (5) can make the filter narrow enough that will yield better feature maps.

The set of features used in this paper are compared to the set of features presented in [5] derived only from the LE measure. The features are given by the mean and the maximum value of the LE feature indexes ΔE_{max}, ΔE, ΔE^1. Also, the performance of the proposed algorithm is compared with the set of features presented in [1] given by the mean and the standard deviation of the filtered image with gabor filters at different orientations and scales. Table 3 shows the comparison of the recognition performance of three approaches using NN and k-nearest neighbored classifiers using 5-folds cross validation procedure. Moreover, the proposed set of features significantly improved the recognition rate. We show that the proposed method exceed the two others methods and the average recognition rate reaches 99.3% while for

the set of features in [5] the recognition system has poor performance explained by recognition rate close to 90%. Also, the method using the mean and the standard deviation of filtered images using Gabor features in [1] gives acceptable performance for expiry date numeral recognition. Figure 12 depicts the comparison results of the performance of the three compared algorithms for each digit composing expiry date code.

Table 3. Comparison of the proposed algorithm with two others methods using 5 folds cross-validations.

Fold	The Method [5]	The Method [1]	The Proposed Algorithm
1	90.2	98.6	98.9
2	89.6	97.8	98.8
3	91	99.1	99.7
4	90.4	98.9	99.6
5	90.8	99.5	99.9
Average	**90.4%**	**98.8%**	**99.3%**

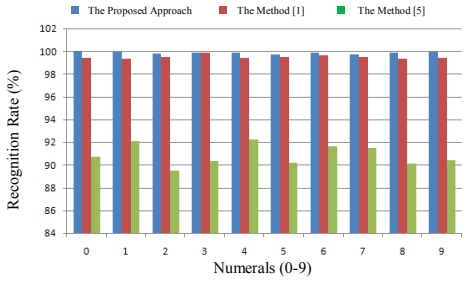

Figure 12. Expiry date numeral recognition rate for three different approaches.

The last series of experiments consists of the performance comparison of MNN and SVM classifier on the same set of features. Table 4 shows the average recognition rate of the two classifiers. It is observed that the recognition rate using SVM is higher than NN MLP and the recognition rate reaches 99.6% and 99.3%, respectively. But, the parameter storage of SVM classifier is significantly expensive compared with MLP neural network. Also, SVM classifier can be working successfully instead of the use of MLP NN for expiration character classification.

Table 4. Comparison of the NN with SVM classifier using different size of features.

Number of Input Features	Average Recognition Rate (%)	
	SVM Classifier	MLP Classifier
33 Input Features	99.6	99.3
42 Input Features	99.4	99.1
51 Input Features	98.9	98.7
69 Input Features	98.6	98.5

4. Conclusions

In this paper, we have presented a vision approach for expiry date numeral recognition using S-Gabor based features and MLP network. The results reported in this paper show that the current set of features can achieve high performance for digit recognition using NN and SVM classifiers. From the results, the proposed approach can be generalized for many computer vision applications. In the others word, the proposed method has two main advantages: The first one is the automation of the recognition process and the second is the high recognition rate for degraded digits. In addition, the use of new set of features derived from S-Gabor filter can be considered encouraging for character recognition. This study is meant to be a seed toward building a recognition system for many printed digits types.

References

[1] Al-Jamimi H. and Mahmoud S., "Arabic Character Recognition using Gabor Filters," *Innovations and Advances in Computer Sciences and Engineering*, Springer Netherlands, pp. 113-118, 2010.

[2] Anagnostopoulos C., Anagnostopoulos I., Loumos V., and Kayafas E., "A License Plate-Recognition Algorithm for Intelligent Transportation System Application," *IEEE Transaction on Intelligent Transportation Systems*, vol. 7, no. 3, pp. 377-392, 2006.

[3] Bigun J. and du Buf J., "Symmetry Interpretation of Complex Moments and the Local Power Spectrum," *Vision Communication Image Representation*, vol. 6, no. 2, pp. 154-163, 1995.

[4] Bovik C., Clark M., and Geisler S., "Multichannel Texture Analysis using Localized Spatial Filters," *IEEE Transactions Pattern Analysis Machine Intelligence*, vol. 12, no.1, pp. 55-73, 1990.

[5] Chan W. and Coghill G., "Text Analysis using Local Energy," *Pattern Recognition*, vol. 34, no. 12, pp. 2523-2532, 2001.

[6] Chang S., Chen L., Chung Y., and Chen S., "Automatic License Plate Recognition," *IEEE Transaction on Intelligent Transportation Systems*, vol. 5, no. 1, pp. 42-53, 2004.

[7] Chiang J., "An Automated Numeral Reading System for VISA Card Application Forms," *Computers in Industry*, vol. 35, no. 2, pp.175-183, 1998.

[8] Duan T., Du T., Phuoc T., and Hoang N., "Building an Automatic Vehicle License Plate Recognition System," *in Proceedings of International Conference on Computer Science*, Atlanta, USA, pp. 59-63, 2005.

[9] Gazzah S. and Amara N., "Networks and Support Vector Machines Classifiers for Writer Identification using Arabic Script," *the International Arab Journal of Information and Technology*, vol. 5, no. 1, pp. 92-101, 2008.

[10] Heikkonen J. and Mantynen M., "A Computer Vision Approach To Digit Recognition on Pulp Bales," *Pattern Recognition Letters*, vol. 17, no. 4, pp. 413-419, 1996

[11] Heitger F., Rosenthaler L., Heydt R., Peterhans E., and Kubler O., "Simulation of Neural Contour Mechanisms: From Simple to End-Stopped Cells," *Vision Research*, vol. 32, no. 5, pp. 963-981, 1991.

[12] Jain A. and Farrokhnia F., "Unsupervised Texture Segmentation using Gabor Filters," *in Proceedings of International Conference on*

Systems, *Man and Cybernetics*, California, USA, pp. 14-19, 1990.
[13] Jiao J., Ye Q., and Huang Q., "A Configurable Method for Multi-Style License Plate Recognition," *Pattern Recognition*, vol. 42, no. 3, pp. 358-369, 2009.
[14] Kovesi P., "Image Features from Phase Congruency," *Videre*: *Journal of Computer Vision Research*, vol. 1, no. 3, pp. 1-26, 1999.
[15] Malamas E., Petrakis E., Zervakis M., Petit L. and Legat J., "A Survey on Industrial Vision Systems Applications and Tools," *Image and Vision Computing*, vol. 21, no. 2, pp. 171-188, 2003.
[16] Palacios R. and Gupta A., "A System for Processing Handwritten Bank Checks Automatically," *Image and Vision Computing*, vol. 26, no. 10, pp. 1297-1313, 2008.
[17] Robbins B. and Owens R., "2D Feature Detection via Local Energy," *Image and Vision Computing*, vol. 15, no. 5, pp. 353-368, 1997.
[18] Sedighi A. and Vafadust M., "A New and Robust Method for Character Segmentation and Recognition in License Plate Images," *Expert Systems with Applications*, vol. 38, no. 11, pp. 13497-13504, 2011.
[19] Shanthi N. and Duraiswamy K., "A Novel SVM-Based Handwritten Tamil Character Recognition System," *Pattern Analysis and Applications*, vol. 13, no. 2, pp. 173-180, 2010.
[20] Simona E., Petkov N., and Kruizinga P., "Comparison of Texture Features based on Gabor Filters," *IEEE Transactions on Image Processing*, vol. 11, no. 10, pp. 1160-1167, 2002.
[21] Sun C. and Si D., "Skew and Slant Correction for Document Images using Gradient Direction," *in Proceedings of the 4th International Conference on Document Analysis and Recognition*, Ulm, Germany, pp. 142-146, 1997.
[22] Sung J., Bang Y., and Choi S., "A Bayesian Network Classifier and Hierarchical Gabor Features for Handwritten Numeral Recognition," *Pattern Recognition Letters*, vol. 27, no. 1, pp. 66-75, 2005.
[23] Suresh V., Kumar M., and Rajagopalan A., "Super Resolution of License Plates in Real Traffic Videos," *IEEE Transactions on Intelligent Transportation Systems*, vol. 8, no. 2, pp. 321-331, 2006.
[24] Valveny E. and Lopez A., "Numeral Recognition for Quality Control of Surgical Sachets," *in Proceedings of the 7th International Conference on Document Analysis and Recognition*, Washington, USA, pp. 379-383, 2003.
[25] Wu W., Liu Z., Chen M., Yang X., and He X., "An Automated Vision System for Container-Code Recognition," *Expert Systems with Applications*, vol. 39, no. 3, pp. 2842-2855, 2012
[26] Youssef S. and AbdelRahman S., "A Smart Access Control using an Efficient License Plate Location and Recognition Approach," *Expert Systems with Applications*, vol. 34, no. 1, pp. 256-265, 2008.

Ahmed Zaafouri received the BSc degree in electrical engineering from the High school of sciences and techniques of Tunis, the MS degree in automatic from same school respectively in 2004 and 2006. Currently, he is an assistant professor in high institute of applied mathematics and informatics of Kairouan. He has published about 10 research papers in many journal and international conferences. His research interests are focused on computer vision, artificial intelligence, pattern recognition and neural networks.

Mounir Sayadi received the BSc degree in electrical engineering from the High school of sciences and techniques of Tunis, the DEA degree in Automatic and Signal Processing from same school and the PhD degree in signal processing from the National School of engineers of Tunis, respectively in 1992, 1994 and 1998. He is currently an Associate Professor at the High school of sciences and techniques of Tunis. He has published over 40 scholarly research papers in many journals and international conferences. He was the Technical Program Co-Chairman of the IEEE International Conference on Industrial Technology, 2004, Tunisia. His research interests are focused on signal and image processing, classification and segmentation.

Farhat Fnaiech received the BSc degree in mechanical engineering in 1978 from Ecole Sup des Sciences et Techniques of Tunis and the master degree in 1980, The PhD degree from the same school in Electrical Engineering in 1983 and the Doctorate Es Science in Physics form the Sciences Faculty of Tunis in 1999. He is currently Professor at the High school of sciences and techniques of Tunis. Pr Fnaiech is Senior Member IEEE and has published over 150 research papers in many Journals and International Conferences. He was the general chairman and member of the International Board Committee of many International Conferences. His is Associate Editor of IEEE Transactions Industrial Electronics. He is serving as IEEE Chapter committee coordination sub-committee delegate of Africa Region 8. His main interest research areas are nonlinear adaptive signal processing, nonlinear control of power electronic devises, digital signal processing, image processing, intelligent techniques and control.